pumps and vacuum valves. Vacuum chamber must be very smooth. HOM absorbers must be installed in every region that has unavoidable discontinuity of the vacuum chamber. Maximum attention to the RF seals designs. Design of a BPM button would contain a cooling possibility. No open (to the beam) ceramic or ferrite tiles. Increase the bunch length as possible. We don't have to forget that beam pipe heating due to resistive-wall wake fields make the beam pipe to be water cooled.

2.10.4 **References**

16. M. Benedikt and F. Zimmermann, "Towards future circular colliders", J. Korean Phys. Soc. 69, 893 (2016).
17. FCC week 2017, Berlin, Germany, https://indico.cern.ch/event/556692/timetable/#20170531.detailed
18. A. Novokhatski, J. Seeman, and M. Sullivan, Analysis of the wake field effects in the PEP-II storage rings with extremely high currents, Nucl. Instrum. Methods Phys. Res., Sect. A 735, 349 (2014).
19. A. Novokhatski, J. Seeman, M. Sullivan, and U. Wienands, Electromagnetic waves excitation, propagation and absorption in the high current storage rings, IEEE Trans. Nucl. Sci. 63, 812 (2016).
20. E. Belli, M. Migliorati, G. Castorina, B. Spataro, M. Zobov, A. Novokhatski, S. Persichelli, "Coupling Impedances and Collective Effects for FCC-ee", Proceedings of IPAC2017, Copenhagen, Denmark, THPAB020, p. 3734.
21. A. Novokhatski, M. Sullivan, E. Belli, M. Gil Costa and R. Kersevan, "Unavoidable trapped mode in the interaction region of colliding beams", Phys. Rev. Accelerators and Beams 20, 111005 (2017)

2.11 Final twin quadrupole design for the FCC-ee based on the canted cosine theta concept

M. Koratzinos
Mail to: m.koratzinos@cern.ch
University of Geneva, Switzerland.

2.11.1 **Introduction**

The FCC-ee is part of the FCC study [1], an ambitious post-LHC accelerator complex study in the Geneva area. FCC-ee is a powerful e^+e^- circular collider with ultimate luminosity performance. This is achieved partly through extremely small vertical emittances of around 1pm. The FCC-ee interaction region [2] is very challenging, in part because the final focus quadrupoles, 2.2 m from the interaction point (IP) sit very close to each other. The field quality of these magnets needs to be excellent and in any case better than one unit of 10^{-4}. The angle between the 30 mm diameter beam pipes of the electrons and positrons is 30 mrad in the horizontal plane, translating to a distance between the centres of the two quadrupoles at the tip of 6.6 cm. This calls for a very compact design, which also needs to have very high field quality. The use of iron to shield the magnetic field of the neighbouring quadrupole can only work at low fields. For the fields needed here (100 T/m field gradient) the iron will saturate and important cross talk would be present. For this reason we have concentrated on an iron-free design and have developed a technique of designing-out field imperfections due to cross talk and edge effects using the canted-cosine-theta (CCT) concept.

CCT magnets have been known since the seventies [1], however only recently have they become popular with magnet designers [3], due to the advent of modern manufacturing techniques (CNC machines and 3D printing). The CCT design concept is based around a pair of conductors wound and powered such that their transverse field components sum up and their axial (solenoidal) fields cancel. In practice the conductor is wound on a pre-cut groove in a supporting hollow cylinder or *mandrel*. The area between grooves is referred to as the *rib* and the supporting solid substrate the *spar*. The difference with a conventional design is that stresses cannot accumulate between conductors but instead forces are intercepted by ribs that transfer the stress to the spar.

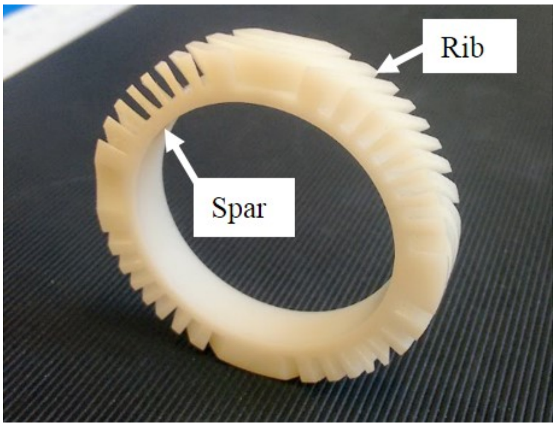

Figure 2: A slice of one of the two layers of a CCT magnet (a quadrupole). The spar is 2 mm wide, followed by a 4 mm rib where the grooves for the cable are located.

In the general case of a coil that produces an arbitrary selection of multipole fields, the centre-line defining the shape of the groove (and the position of the centre of the powered cable) for one of the two coils of the CCT is described by the equation

$$x = R\cos\theta\,;$$

$$y = R\sin\theta\,;$$

$$z = \sum_{n_B}\left[\frac{R\sin(n_B\theta)}{n_B\tan\alpha_{n_B}} + \frac{\omega\theta}{2\pi}\right] + \sum_{n_A}\left[\frac{R\cos(n_A\theta)}{n_A\tan\alpha_{n_A}} + \frac{\omega\theta}{2\pi}\right] \tag{1}$$

Where R is the radius of the coil, A and B are the skew and normal components of the field, n_A and n_B are the skew and normal multipoles ($n_B = 1$ is the dipole component, $n_B = 2$ the quadrupole component, etc., same with $n_A = 1$: skew dipole component, etc.). The angles α_{n_A}, which could be a function of z, are the angles of the groove (or wire) with respect to the horizontal on the mid plane per desired multipole (called the skew angles). An angle of zero would ensure no relevant multipole component. θ runs from 0 to $2\pi n_t$ where n_t is the number of turns. For the second layer, R is slightly increased (depending on the thickness of the spar and the cable) and the skew angle has the opposite sign. The start and end of both layers are located on top of one another. We can see from equation (1) that the groove and cable describe a circle in the x-y plane whereas in the longitudinal (z) direction there is a longitudinal shift parameter ω per revolution, plus the multipole component.

The CCT design offers significant advantages over traditional magnet design for certain applications. Their field quality is excellent due to the purity of the design and due to the fact that the cable grooves can be very precisely machined; they are easy to manufacture using CNC machines or even 3D printing techniques, leading to very fast prototyping; there is no need for coil pre-stress during assembly, leading to simple and fast winding; reduced coil stresses improve magnet training; the design gives total freedom to implement any multipole arrangement, therefore capable of producing compact double aperture magnets with the required field quality, as demonstrated in this paper; and finally this concept uses fewer components and is considerably lighter than traditional designs, leading to reduced overall costs.

The disadvantage of the CCT design is that the two magnet coils work against each other to cancel the longitudinal field, leading to more conductor material per Tesla produced. Since our application is not a high field application, we are not affected by this potential limitation in this design.

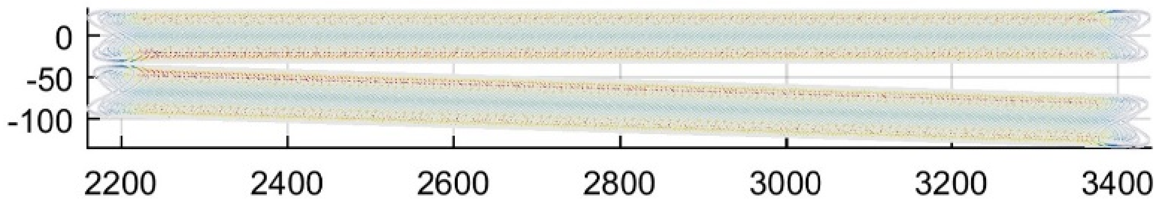

Figure 3: The position of the two QC1L1 magnets, at an angle of 30 mrad and at a distance of 2.2 m from the IP. The axes go through the positron beamline. Horizontal plane. Distances in mm.

2.11.2 **Edges Correction**

2.11.2.1 ***The coil***

The FCC-ee final focus quadrupole comprises six coils [5], three per beam, out of which the most challenging is the QC1L1 pair that sits closer to the IP at a distance of 2200 mm (see Figure 3). Its length is 1200 mm and has an inner bore of 40 mm diameter. The cable of the inner coil has an inner and outer radius of 22 and 26 mm, and the outer coil 28 and 32 mm. The inner spar occupies the area of radius 20 to 22 mm and the middle spar a radius of 26 to 28 mm. The grooves are 2 mm wide and 4 mm high, leaving a possible cross section for the cable of 8 mm^2. The pitch between grooves is 5 mm, leaving a minimum rib width of 1mm. The beam pipe is expected to have a diameter of 30 mm, so all multipoles are calculated at a radius of 10 mm, at an aperture of 2/3. This quadrupole produces a gradient of 100 T/m for a total current of around 5800 A. The transverse components of the magnet can be seen in Figure 4.

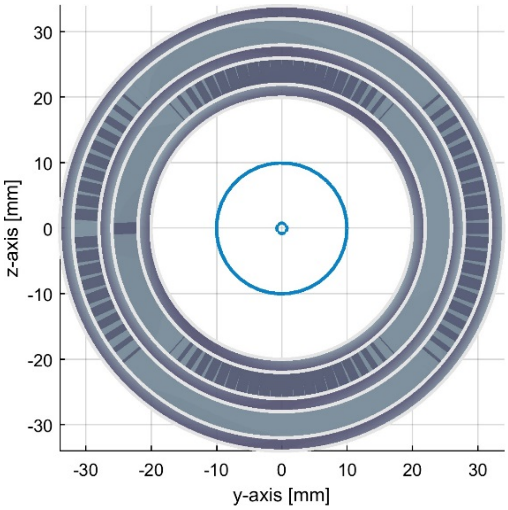

Figure 4: A view in the transverse plane of the quadrupole CCT magnet QC1L1. The blue circle (radius 10mm) is where multipoles are calculated.

The software used throughout this analysis is the Field 2017 suite of programs [6].

The multipole components around both edges of such a magnet can be seen in Figure 5. Only one magnet edge is shown (the one at negative z). The other edge has components which are antisymmetric. All A and B components integrate to zero when integrating over the length of the magnet. However, only the B components integrate to zero locally (per edge). As this magnet will be placed in an area of rapidly varying optics functions, it is beneficial if an edge correction could be applied so that the multipoles would integrate to zero locally.

The integral of the multipole components (normalized to the B2 field, in units of 10^{-4}) can be seen in Figure 6.

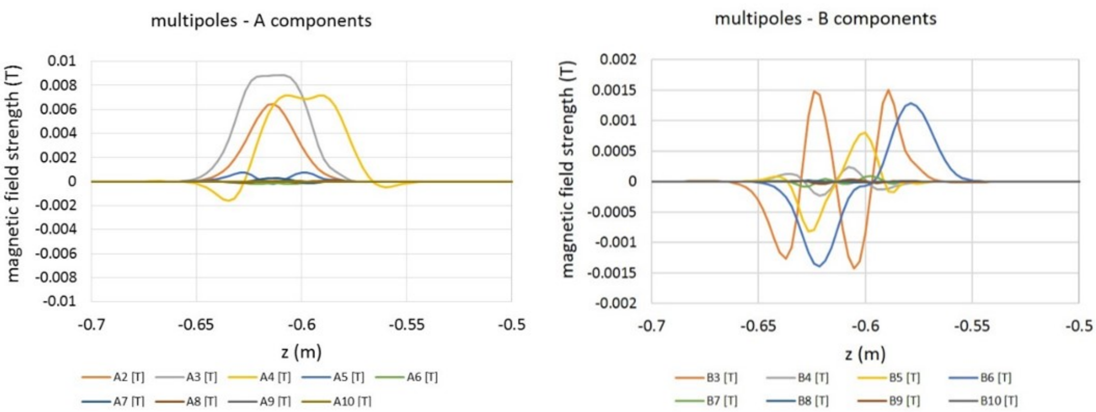

Figure 5: A and B multipole components up to order 10 on the left edge of the coil. The A, B1 and B2 components have been omitted. The right edge has components with a flipped sign.

2.11.2.2 *The correction*

The correction needs to be applied locally to the A components. This is done by applying non-zero multipole components for the first two turns of the coil. To make sure that the cable does not turn back on itself (i.e. that the gap between the adjacent windings of the cable is always larger than zero) the pitch for these first two windings has been increased to 15mm from 5 mm for the rest of the coil. Corrections up to order 6 are performed (for higher orders the residual effect is too small). Following the A corrections, some B component corrections need to be also applied, again for the first two turns of the coil. This analysis is performed in the absence of any alignment or positioning errors. The integrated multipole plot after the correction can be seen in Figure 7. This demonstrates that a correction to an arbitrary degree of accuracy can be achieved (here we have stopped the process when an accuracy of 0.05 units or better had been achieved). The magnitude of the edge corrections can be seen in Table 1.

Table 1: Size of edge correction (in degrees) for the first and last windings of the magnet for all corrected multipoles. B2, the main component, is also given for reference.

	A2	A3	A4	A5	A6	B2	B3	B4	B5	B6
α left	-3.1	19	-38	6	6	60	-5	-3.5	6.5	1.5
α right	3.1	-19	38	-6	-6	60	-5	-3.5	6.5	1.5

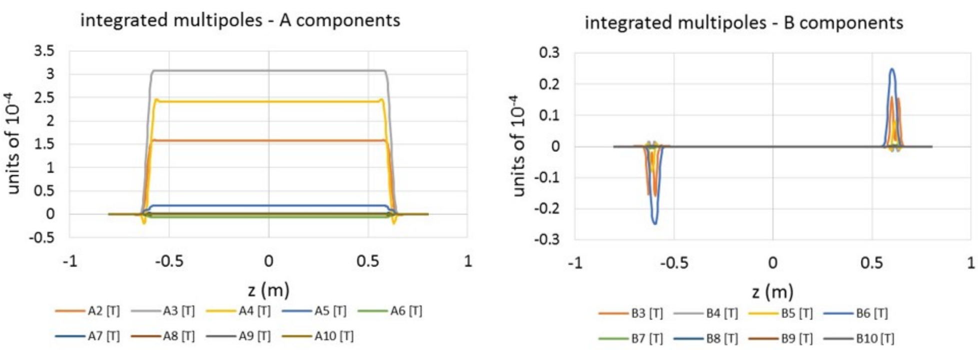

Figure 6: Integrated multipoles, before correction, in units of 10^{-4}. The A1, B1 and B2 components have been left out for clarity. The A1 and B1 components do not need to be corrected, whereas the B2 component has a final integrated value (by definition) of 10,000.

2.11.3 **Crosstalk compensation**

2.11.3.1 ***The coils***

The edges correction is applied to a single coil in standalone mode. However, in the case of the FCC-ee the QC1L1 magnets sit in close proximity and at a variable distance from each other, as seen in Figure 3. Their distance from their magnetic centres is 66 mm at the tip and 102 mm at the end away from the IP (the magnets are 1.2 m long). The FCC-ee final focus system has many more magnetic elements, but we will concentrate on the crosstalk compensation of the two QC1L1 magnets, which is the most challenging problem. No iron is present in the vicinity of the magnets. The two QC1L1 magnets are a mirror image of each other (the hypothetical mirror standing vertically between the two beamlines) and are powdered together by the same power supply.

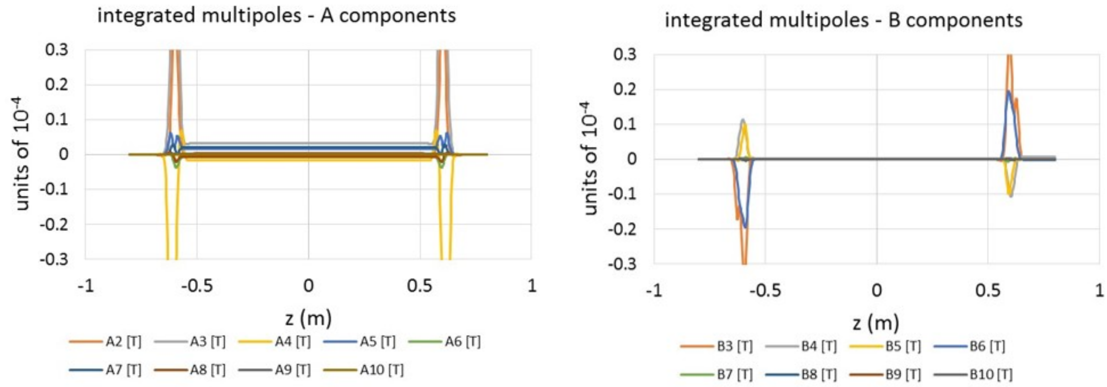

Figure 7: Integrated multipoles in units of 10^{-4} after correction. Note the different scale compared to Figure 6**.**

The uncorrected multipoles from this arrangement can be seen in Figure 8. There are significant components due to the close proximity of the other coil.

2.11.3.2 *The method*

Every effort is made to perform any needed correction locally. Currently the correction is performed empirically, with plans to develop an automated minimization procedure in the near future. Multipole corrections are nearly orthogonal to each other, so the minimization process converges rapidly. Only exception is the edges A2 correction which is affected by other multipoles, therefore the correction for A2 should be performed last.
It is not clear where the limits of the method are with respect to the level of compensation possible. We simply stopped at a level (around 0.05 units) where we felt that other distortions (for instance, due to misalignment or winding errors) would be more important.

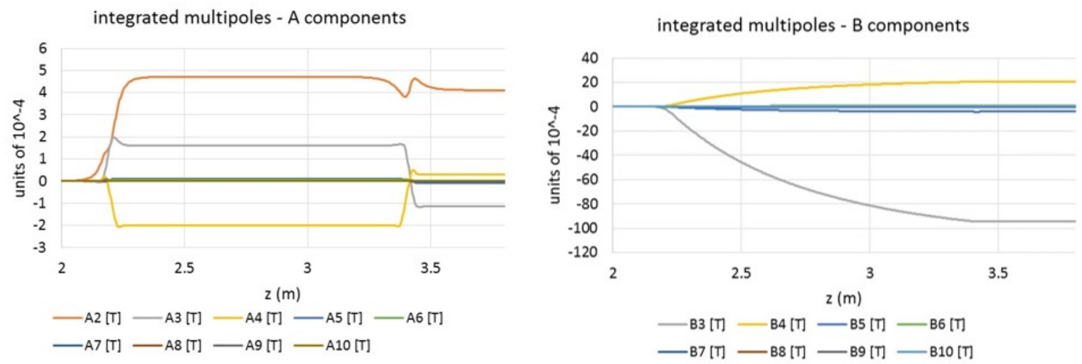

Figure 8: Integrated multipoles in units of 10^{-4} before correction in the case of two side-by-side QC1L1 magnets. As expected from the proximity of the two quadrupoles, the effect of cross talk is large.

2.11.3.3 *The correction*

In contrast to the earlier case, here we need to introduce multipole components along the whole length of the magnet. The results are very encouraging and can be seen in

Figure 9. All multipoles are corrected to within 0.05 units. The maximum and minimum correction along the length of the magnet (excluding the edges where a special correction is performed) can be seen in Table 2.

Table 2: Size of crosstalk correction (in degrees) along the length of the quadrupole. The edges have been excluded from this table. B2, the main component, is also given for reference

	A2	A3	A4	A5	A6	B2	B3	B4	B5	B6
α max	0	0	0	0	0	60	5.1	-4.0	2.0	-1.4
α min	0	0	0	0	0	60	0.8	-0.3	0.1	-0.0

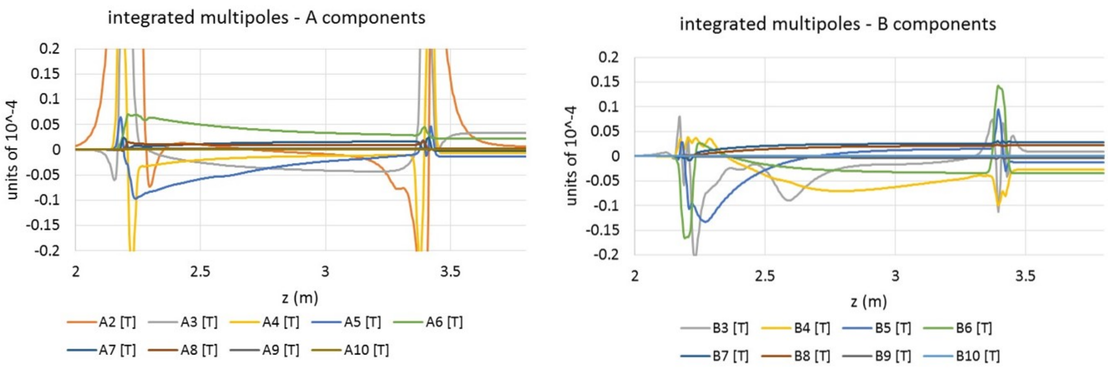

Figure 9: Integrated multipoles in units of 10^{-4} after correction for the effect of crosstalk from the adjacent quadrupole. All multipoles can be corrected to better than 0.05 units

2.11.4 **Conclusions**

The CCT magnet concept offers a versatility seldom associated with magnet design. Any multipole arrangement can be designed and implemented. We have first demonstrated that the inevitable edge effects of our test CCT quadrupole magnet (and therefore any CCT magnet) can be eliminated to below 0.05 units. We have further demonstrated that in an iron-free environment we can create two nearly-perfect parallel powered quadrupoles that have a gap of only 2 mm at one tip and 4 cm at the other. Again, the correction is such that residual multipole components can be kept well below 0.05 units. This design eliminates the need for a large number of corrector magnets and might be important in an application where space is very limited and optics performance very important, like the interaction region of FCC-ee.

2.11.5 **Acknowledgements**

The financial support of ETH Zurich to this work is gratefully acknowledged.

2.11.6 **References**

1. D. I. Meyer and R. Flasck. (n.d.). A new configuration for a dipole magnet for use in high energy physics applications. *NIM A 80.2 (1970), pp 339-341*.
2. F. Bosi et al. (n.d.). Compact Superconducting High Gradient Quadrupole Magnets for the Interaction Regions of High Luminosity Colliders. *IEEE Transactions on Applied Superconductivity, VOL. 23, NO. 3, JUNE 2013*.

3. J. van Nugteren. (2011). *Internship Report: CERN, Software development for the Science and Design behind Superconducting Magnet Systems.* tech. rep., Twente University: Energy Materials and Systems and CERN: ATLAS magnet team.
4. M. Koratzinos et al. (THOPOR023). The FCC-ee Interaction Region Magnet Design. *IPAC 2016.* Busan, Korea.
5. S. Caspi. (n.d.). Design, Fabrication and Test of a Superconducting Dipole Magnet Based on Tilted Solenoids. *IEEE Trans. Appl. Supercond. 17.2 (2007), pp. 2266-2269.*
6. The FCC-ee study. (n.d.). http://cern.ch/fcc . Retrieved from http://cern.ch/fcc

2.12 Proposed RF Staging Scenario for FCC-ee

O. Brunner, A. Butterworth, I. Karpov, S. Aull, N. Schwerg
CERN, Geneva, Switzerland
(Dated: November 15, 2017)

2.12.1 **Introduction**

FCC-ee is a proposed high-energy electron positron circular collider that could initially occupy the 100-km tunnel of the future 100 TeV FCC-hh hadron collider. The parameter range for the e+e− collider is large, operating at center-of-mass energies from 90 GeV to 365 GeV with beam currents ranging between 1.39 A and 5.4 mA, at fixed synchrotron radiation power of 50 MW per beam. These are challenging parameters for the radiofrequency (RF) system because of the extreme voltage requirements and beam loading conditions. This document details a scenario for gradual evolution of the FCC-ee complex by step-wise expansion and reconfiguration of the superconducting RF system.

2.12.2 **Operation model**

The main center-of-mass operating points with large physics interest are around 91 GeV (Z-pole), 160 GeV (W pair production threshold), 240 GeV (Higgs resonance) and 365 GeV (above top-antitop (ttbar) threshold). The construction of FCC-ee will therefore proceed in five steps, combining eight months of operation periods with four months of interleaved winter shutdowns during which the hardware upgrades for energy increase can take place.

In order to collect the required luminosity and allow for interesting physics at each energy step, it is planned to run the machine four years at the Z-pole, one year at the W pair production threshold, three years at the Higgs resonance and finally four years at the highest energy, one year at the ttbar threshold, followed by three years at 182.5 GeV per beam. The main machine parameters are summarized in Table 1 [1].